Increased Melting of Marine-Terminating Glaciers by Sediment-Laden Plumes

Craig McConnochie[1] and Claudia Cenedese[2]

[1]University of Canterbury
[2]Woods Hole Oceanographic Institution

November 22, 2022

Abstract

This paper summarizes the results of the first investigation into the effect of particle-laden plumes on glacier melting using laboratory experiments. We find that the melt rate, when the ice is exposed to a particle-laden plume, can be increased by up to 60% compared to when the ice is exposed to an equivalent plume without particles. The increased melt rate is linked to increased entrainment into the turbulent plume, demonstrating a link between turbulent entrainment and the melt rate of the ice face. We use this link to propose a modification to the commonly used 'three-equation model' that explicitly accounts for variations in entrainment rates.

Increased Melting of Marine-Terminating Glaciers by Sediment-Laden Plumes

C. D. McConnochie[1] and C. Cenedese[2]

[1]Department of Civil and Natural Resources Engineering, University of Canterbury
[2]Physical Oceanography Department, Woods Hole Oceanographic Institution

Key Points:

- Submarine melting of an ice face can be increased by the presence of sediment in a subglacial discharge plume
- The increased melting is due to increased entrainment into the plume, showing a direct link between entrainment and melting
- A modification to a common submarine ice melting parameterization is proposed which accounts for the link between entrainment and melting

Corresponding author: Craig McConnochie, `craig.mcconnochie@canterbury.ac.nz`

Abstract

This paper summarizes the results of the first investigation into the effect of particle-laden plumes on glacier melting using laboratory experiments. We find that the melt rate, when the ice is exposed to a particle-laden plume, can be increased by up to 60% compared to when the ice is exposed to an equivalent plume without particles. The increased melt rate is linked to increased entrainment into the turbulent plume, demonstrating a link between turbulent entrainment and the melt rate of the ice face. We use this link to propose a modification to the commonly used 'three-equation model' that explicitly accounts for variations in entrainment rates.

Plain Language Summary

Ice loss from the Greenland ice sheet is more rapid in locations where fresh water is released at the base of marine terminating glaciers. The fresh water forms a buoyant plume that rises vertically next to the ice face. Previous observations of these plumes have shown that they can contain significant concentrations of suspended sediment. We show, using laboratory experiments, that the melt rate of a vertical ice face is increased by up to 60% by the presence of suspended particles in the vertically rising plume. This observation suggests that the effect of such plumes could be larger than current modelling studies predict. Finally, we suggest an adjustment to those models such that the effects of sediment-laden plumes can be fully accounted for.

1 Introduction

Ice loss from the Greenland Ice Sheet is currently a major contributor to global sea level rise. Approximately half of this ice loss is due to the calving of icebergs with the remainder due to direct melting of marine-terminating glaciers into the ocean (Rignot et al., 2013). Although the melt rate has been increasing over recent years (Pritchard et al., 2009), there remains a large uncertainty in predictions of future melt rates. Increasing our understanding of glacier melt rates and associated drivers, enables better predictions of future sea level rise and better planning decisions to be made.

For both calving of icebergs and direct melting of the ice sheet, the interaction between the ocean and the ice face is crucial. The ocean provides a source of heat and salt to the ice, the transport of which directly determines the melt rate of the ice face (Jenkins, 2011; Kerr & McConnochie, 2015). However, the transport process itself is highly complex and involves both relatively large-scale turbulent processes and small-scale molecular processes.

A commonly used numerical parameterization developed to predict the melt rate of an ice face based on the bulk temperature, salinity and velocity close to the ice is known as the 'three-equation model' (e.g. Jenkins, 2011). Both the turbulent and molecular transport processes are parameterized by constant transfer coefficients to give the flux of heat and salt to the ice face. These transfer coefficients will hereafter be referred to collectively as $\Gamma_{\mathrm{T,S}}$.

Due to the relatively warm air temperatures in Greenland over summer, a significant amount of surface melting of the ice sheet occurs. The surface meltwater sinks to the base of the ice sheet and flows beneath glaciers to the grounding line — the location where a glacier becomes afloat (Nienow, 2017). At the grounding line, the meltwater is released into the ocean and forms a highly vigorous turbulent plume that rises along the ice face (Fried et al., 2015; Straneo & Cenedese, 2015). The dynamics of subglacial plumes have received a large amount of attention over recent years as they are often associated with elevated melt rates (see Straneo & Cenedese, 2015).

As the surface meltwater flows beneath the ice sheet it can erode significant amounts of sediment. As a result, subglacial plumes contain high sediment concentrations and can often be observed from surface photographs when they reach the surface (Mankoff et al., 2016). Recent experimental work has shown that the entrainment of ambient water into an axisymmetric turbulent plume is increased by up to 40% when the plume contains suspended dense sediment (McConnochie et al., 2021). Given that the transport of heat and salt to the ice face occurs mainly by entrainment of ambient fluid into the subglacial plumes, it could be expected that the sediment contained in subglacial plumes would enhance the melt rate of the glacier. In contrast, the three-equation model would predict reduced melt rates as higher rates of entrainment will cause the plume to decelerate more rapidly and reduce the parameterized transport of heat and salt. This contradiction leaves it unclear how the suspended sediment carried in subglacial plumes will affect the melt rate of a glacier face and how such effects should be included in numerical models.

In this paper we present laboratory experiments of a vertical ice face melting in contact with a particle-laden plume. Section 2 contains a description of the experimental apparatus and procedure. Experimental results are presented in Section 3 before a discussion of the implications for modelling ice-ocean interactions is provided in Section 4.

2 Methods

Experiments were conducted in a glass walled tank that was 150 cm long, 15 cm wide and 30 cm high and is shown schematically in Figure 1a. The tank was stored in a temperature controlled room that was kept at approximately 3 °C. The tank was initially filled to a depth of 25 cm with oceanic salt water that had been left in the room to thermally equilibrate for at least 24 hours prior to the experiment.

In all experiments, the ambient fluid temperature and salinity were $3.2 \pm 0.2\,^{\circ}\mathrm{C}$ and $3.35{\pm}0.05$ wt.%, respectively. The plume fluid is supplied to the base of the ice block with a flow rate Q_s of $6.0{\pm}0.1\,\mathrm{cm}^3\,\mathrm{s}^{-1}$ and fluid is removed from the tank at the same flow rate from the opposite end. The buoyancy flux due to the subglacial discharge is approximately 25 times that due to the melting of the ice face such that the buoyancy flux of the plume can be assumed to be constant with height and dominated by the source buoyancy flux (McConnochie & Kerr, 2017a). Particles fall out from the surface current (Figure 1) with a settling velocity v_s which is significantly smaller than the velocity of the rising plume next to the ice.

The ice used in the experiments was made from fresh water with a small amount of blue food dye added for visualization. The fresh water was left at room temperature for at least 48 hours prior to being frozen so that the ice was free of air bubbles. The water was frozen in a mould in a freezer for at least 48 hours until it came to a uniform temperature. The mould was constructed such that the width of the ice block was slightly smaller than the width of the tank so the ice block could be smoothly placed in, and removed from, the tank. Although this resulted in a very thin layer of fluid being trapped between the ice block and the tank wall, this did not appear to result in further convection and the melting against the sides of the tank was negligible. Prior to the experiment the ice was removed from the mould and placed in the temperature controlled room for 90 minutes. During this time the ice began to warm up but didn't start melting which ensured that almost all of the heat flux to the ice during an experiment resulted in melting of the ice rather than warming, and that the measured melt rate was approximately

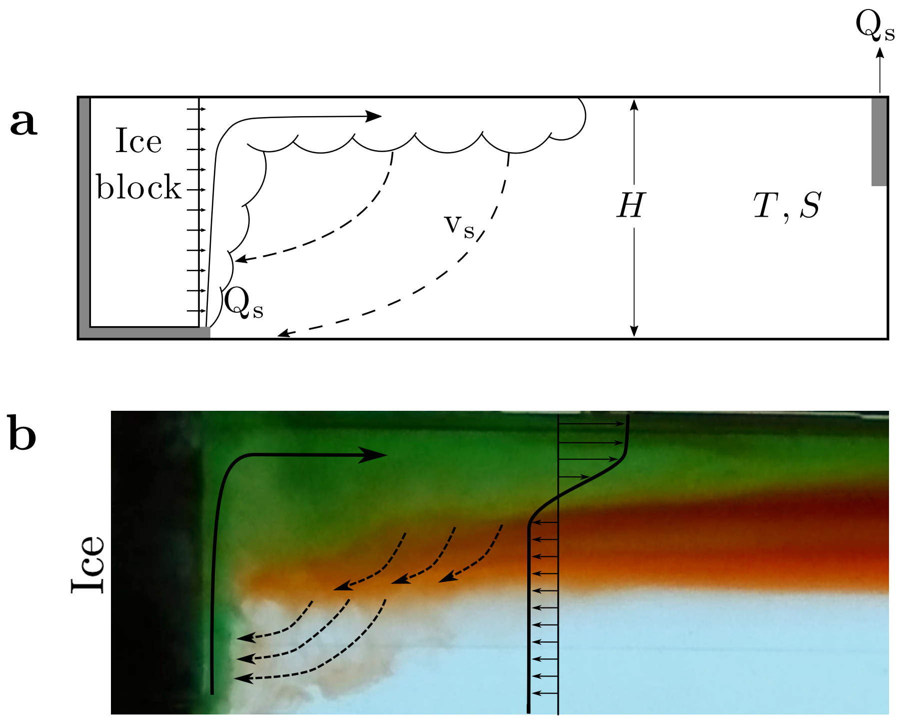

Figure 1. **a)** A schematic of the tank used in the experiments. The tank is filled to a depth H with ambient fluid of temperature T and salinity S and an ice block is placed against one end wall. The plume fluid is supplied to the base of the ice block with a flow rate Q_s and drawn out of the tank with the same flow rate from the opposite side. Particles fall from the surface buoyant current with a settling velocity v_s which is significantly smaller than the velocity of the rising plume next to the ice.

b) A photograph taken from a qualitative experiment of the top-left section of the tank. The source fluid was dyed green and a layer of fluid close to the surface at the start of the experiment was dyed red. The light red region in the bottom half of the tank indicates particles settling and being drawn back to the ice face due to turbulent entrainment. The light red color is caused by the transport of some ambient water by the settling particles.

proportional to the total heat flux to the ice. Immediately before placing the ice in the tank it was dried and weighed on a scale.

During an experiment, a fresh water line plume was produced at the base of the ice block. The line plume was produced from an array of ten point sources equally spaced across the width of the tank. Each source was designed to generate a turbulent plume at the exit location (Kaye & Linden, 2004) and the individual plumes quickly merged to form a line plume. The melt rate of the ice block was observed to be higher above the source locations along the bottom 1–2 cm of the ice block. Above this height the melt rate was spatially uniform, suggesting that the velocity of the plume was also spatially uniform — i.e. that the plume was two-dimensional.

The plume source fluid was fresh water that had been stored in the cold room for 24 hours. Prior to the experiment small ice cubes were added to the source fluid to reduce the temperature of the fluid to between 0.5 and 1.0 °C. The exact temperature of the source fluid was measured to within ±0.1 °C with an alcohol thermometer immediately prior to an experiment. Immediately before an experiment the ice cubes were removed, food dye was added to the fresh water for visualization and the desired mass of particles was added to the fluid. These particles were kept in suspension during an experiment by continually stirring the source fluid.

The particles used were solid glass microspheres with a density of $2.5\,\mathrm{g/cm^3}$ and diameters of 38–53 μm. During an experiment the plume fluid containing the particles rose vertically along the ice face before spreading as a buoyant surface current. As the plume fluid spread along the surface, particles settled from the surface current and were drawn back towards the ice face due to the entrainment of ambient fluid into the plume (Figure 1).

Each experiment was run for approximately 5 minutes. After this time, the ice block face started to retreat behind the position of the source and the height where the plume became attached to the ice face began to shift upwards. At the conclusion of an experiment the ice was removed from the tank, dried, and weighed. The loss of mass during an experiment was used to estimate the melt rate based on a density of ice of $0.92\,\mathrm{g\,cm^{-3}}$ and assuming that the melting was uniformly distributed over the ice face that was exposed to the particle-laden plume.

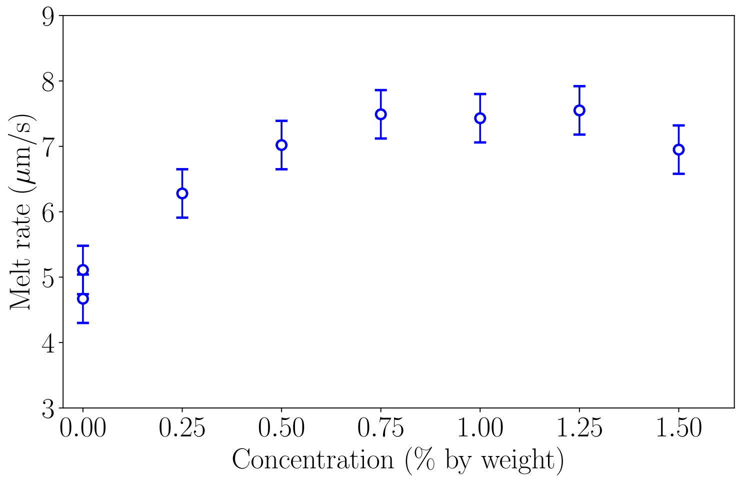

Figure 2. Measured melt rate as a function of sediment concentration by weight.

Figure 1b shows a photo from a qualitative experiment. A freshwater subglacial line plume (dyed green) was produced at the base of an ice block (dyed blue) which rose vertically and spread horizontally once it reached the free surface. Experiments were carried out with different concentrations of particles added to the subglacial plume. Similarly to the experiments presented in Sutherland et al. (2020), particles are expected to settle from the horizontally flowing surface current before being drawn back towards the ice face by entrainment of ambient fluid into the plume (dashed lines in Figure 1a and b).

3 Results

The measured melt rate is shown in Figure 2 as a function of sediment concentration by weight. The estimated uncertainty shown in Figure 2 is the difference between two repeated experiments without particles. Figure 2 clearly shows that the melt rate of the ice block is strongly dependent on the sediment concentration. Furthermore, this dependence appears to be complex and non-linear. At low particle concentrations, the measured melt rate increases rapidly with the particle concentration until the melt rate is approximately 60% larger than that without added particles. However, further increasing the particle concentration has no effect on the measured melt rate.

As in McConnochie et al. (2021), we attempt to understand this non-linear response by characterizing the particle concentration by a buoyancy flux ratio, P. The buoyancy

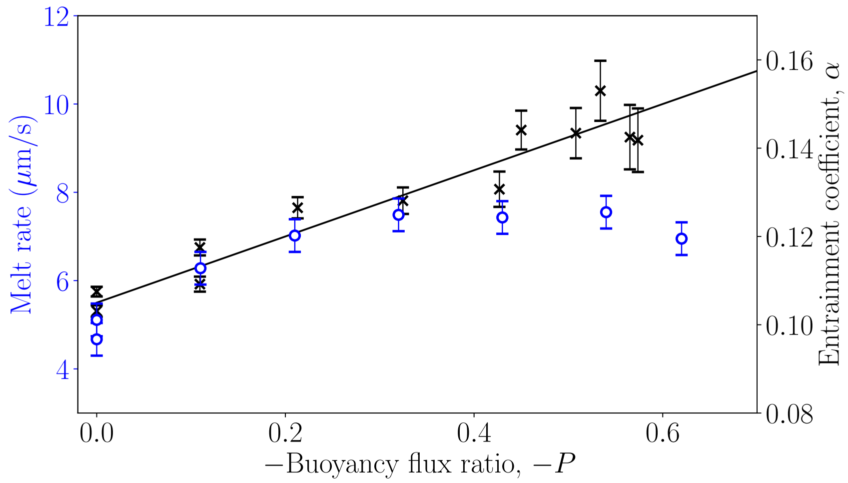

Figure 3. Measured melt rate (blue circles, left axis) and the entrainment coefficient estimated by McConnochie et al. (2021) (black crosses, right axis) plotted against the buoyancy flux ratio. Also shown is an empirical fit to the entrainment coefficient (black line, right axis) from McConnochie et al. (2021) given by $\alpha = 0.105 - 0.75P$.

flux ratio compares the component of the source buoyancy flux that is due to the particles, B_{part}, with the buoyancy flux due to the temperature and salinity induced density differences between the plume and the ambient fluid, B_{fluid}:

$$P = \frac{B_{\text{part}}}{B_{\text{fluid}}}. \tag{1}$$

Here the buoyancy flux is defined as

$$B = Q_0 g \left(\frac{\rho_a - \rho_0}{\rho_a} \right) \tag{2}$$

where Q_0 is the plume volume flux at the source, g is the acceleration due to gravity, ρ_a is the ambient fluid density, and ρ_0 is the source fluid density. The total source buoyancy flux is the given by $B_{\text{part}}+B_{\text{fluid}}$, and $P = 0$ corresponds to a plume with no particles while $P = -1$ corresponds to a plume where the particle buoyancy is exactly balanced by the fluid buoyancy. Note that $P \leq 0$ since the buoyancy flux due to the particles is downwards while the buoyancy flux due to fluid density differences is upwards.

On Figure 3 we show the same measurements of melt rate that were shown on Figure 2 but plotted against the buoyancy flux ratio instead of the particle concentration. Estimates of the entrainment coefficient with an empirical fit through the data, both from McConnochie et al. (2021), are also shown on Figure 3. Results from McConnochie et al. (2021) are only shown for those experiments that had a particle size equal to that used in the present study. The entrainment coefficient is defined as $\alpha = U_e/U$, where U_e is the velocity with which ambient fluid is entrained into the plume and U is the characteristic plume velocity (Morton et al., 1956).

Figure 3 shows a clear relationship between the melt rate and the entrainment coefficient. McConnochie et al. (2021) suggested that the entrainment coefficient increases linearly with the buoyancy ratio. We find that the melt rate also increases linearly with the buoyancy ratio, up to some limit where it becomes insensitive to further increases. From the data of McConnochie et al. (2021), it remains unclear if the entrainment coefficient also reaches a maximum value, or would do so at larger values of $-P$. We note that the plume in this study was a two-dimensional line plume whereas that used in McConnochie et al. (2021) was an axisymmetric plume. Although we expect the dependence of the entrainment coefficient on the buoyancy flux ratio to be similar, the different geometries could explain the difference between the melt rate and the entrainment coefficient at large values of $-P$.

Although the present experiments were conducted with a single buoyancy flux and a single particle size, we expect the results to hold provided the particle size is sufficiently small, and the buoyancy flux is sufficiently large, that individual particles do not settle from the turbulent plume. McConnochie et al. (2021) showed that the entrainment coefficient is only a function of the particle concentration and does not depend on the buoyancy flux or the particle size (at least within a range of particle sizes). However, as previously observed, increasing the source buoyancy flux of the plume will increase the velocity of the plume and hence the melt rate (McConnochie & Kerr, 2017a). The dependence of the melt rate on the buoyancy flux is separate from the dependence on the entrainment coefficient illustrated in Figure 3 and is expected to be unchanged with little interaction between the two processes.

4 Discussion

4.1 Implications For Modelling the Melt Rate

The results of this study show, for the first time, a direct link between the entrainment of ambient fluid into a turbulent plume and the melting of an ice face. This link is not entirely unexpected as both processes involve turbulent transport from the ambient fluid into the plume. However, the result is also not obvious. Turbulent entrainment involves the movement of irrotational fluid across a vorticity interface located at the edge of a plume. In contrast, melting of the ice face involves scalar transport of heat and salt due to both turbulent processes across the plume and molecular processes across a small but important laminar sublayer next to the ice face (Wells & Worster, 2008; McConnochie & Kerr, 2017b). Given the close link between turbulent entrainment and the melt rate of an ice face (Figure 3), it becomes clear that the melt rate should depend on all factors that affect turbulent entrainment, not only the presence and concentration of suspended sediment. These potentially important factors include the geometry of the flow and the nature of the buoyancy source.

Current understanding of the effect of subglacial plumes on glacial melting implies that subglacial plumes increase the melt rate of an ice face by increasing the flow velocity next to the ice. Although this mechanism is undoubtedly important, the direct link between entrainment and melting introduces new processes whereby subglacial plumes could affect the melt rate of an ice face. The entrainment coefficient of a point source plume originating from the base of an ice face is expected to be different to that of a plume from a line source (Richardson & Hunt, 2022). Thus, the initial geometry of the subglacial discharge will influence the melt rate of an ice face (Cenedese & Gatto, 2016; Slater et al., 2015), even in cases where the velocity next to the ice is identical.

The entrainment coefficient of a plume adjacent to an ice face will also depend on whether the plume buoyancy flux is dominated by that of the subglacial discharge or by that due to the release of fresh water due to melting (McConnochie & Kerr, 2017a). Which source of buoyancy is dominant will change with height (as increasing amounts of meltwater are released) and seasonally (as the subglacial discharge flux changes). Therefore, the entrainment coefficient, and hence the melt rate, is expected to vary both seasonally and with depth. We note again that the impact on the entrainment coefficient is separate from the direct impact that changing the subglacial discharge flux will have on the plume velocity.

A related question to that asked here is whether the presence of bubbles in a subglacial plume could have a similar impact on the melt rate as the presence of suspended sediment does. These bubbles could plausibly enter the subglacial plume due to gas that was initially frozen into the ice being released as it melts. Laboratory experiments have found that bubbles frozen into the ice do not affect the melt rate of the ice (Josberger, 1980), and this is not expected to change at a geophysical scale. The different behaviour with bubbles and solid particles can be explained by previous studies that have shown that, provided the rise velocity of the bubbles is smaller than that of the plume, bubble plumes behave much like single-phase plumes (Mingotti & Woods, 2019). In addition, the dependence of the entrainment coefficient on the buoyancy flux ratio shown in Figure 3 was not observed when the particle buoyancy and the fluid buoyancy acted in the same direction and $P > 0$ (McConnochie et al., 2021), as would be the case if the particles in a subglacial discharge were replaced with bubbles.

4.2 Updated Melting Parameterization

Currently the three-equation model parameterizes the transport of heat and salt through constant transfer coefficients which are multiplied by the flow velocity and a constant drag coefficient (see Jenkins, 2011). However, the present study shows that it is the entrainment velocity, rather than the flow velocity, that governs the transport of heat and salt, suggesting that modifications need to be made to the parameterization. We propose redefining the scalar transfer coefficients, $\Gamma_{\mathrm{T,S}}$, to more accurately and explicitly represent the two factors that affect the transport of heat and salt to the ice face:

$$\Gamma_{\mathrm{T,S}} \equiv \alpha\hat{\Gamma}_{\mathrm{T,S}}. \tag{3}$$

Here we have separated the traditional transfer coefficients, $\Gamma_{\mathrm{T,S}}$, into two new components. The first is the entrainment coefficient, α, and the second is an updated transfer coefficient, $\hat{\Gamma}_{\mathrm{T,S}}$, which acts upon the entrainment velocity rather than the flow velocity:

$$Q_{\mathrm{T,S}} = C_D^{1/2} U \Gamma_{\mathrm{T,S}} \Delta_{\mathrm{T,S}} = C_D^{1/2} \alpha U \hat{\Gamma}_{\mathrm{T,S}} \Delta_{\mathrm{T,S}}, \tag{4}$$

where $Q_{\mathrm{T,S}}$ is the flux of heat or salt, C_D is the drag coefficient, and $\Delta_{\mathrm{T,S}}$ is the driving temperature or salinity difference. The advantage of this new formulation is that it explicitly includes the relationship between the transport of heat and salt to the ice face and the entrainment coefficient, while still allowing the scalar transport coefficients to take constant values.

Equation (3) can be easily implemented into the three-equation model and does not require the knowledge of additional parameters since the entrainment coefficient is typically already used in a coupled plume model to determine the flow velocity (Jenkins, 2011). However, it importantly accounts for the fact that the entrainment coefficient will have different values in different situations based on the plume source geometry (Cenedese & Linden, 2014; Richardson & Hunt, 2022) and sediment concentration (McConnochie et al., 2021). The improved parameterization, (3), allows the dependence of the melt rate on the entrainment coefficient, clearly shown for the first time in this paper, to be easily included in numerical models. As such the true effect of subglacial plumes, including the effects of suspended sediment and geometric effects, on the melting of marine terminating glaciers can be modelled.

5 Conclusion

Novel laboratory experiments have shown, for the first time, that submarine melting of marine-terminating glaciers can be enhanced by up to 60% by the presence of sediment in a subglacial discharge plume. The experiments have also shown a direct link between entrainment into a turbulent plume rising next to an ice face and the melt rate of that ice face. In addition to the effect of suspended sediment, this link implies that other plume properties that affect the rate of entrainment, such as the source geometry, will also affect the melt rate of the ice face.

To account for these differences, we propose that the entrainment coefficient of a turbulent plume be explicitly included in parameterisations of submarine ice melting (the three-equation model). This can be done by redefining the turbulent transfer coefficient so that it doesn't (implicitly) include the entrainment coefficient of the plume. Doing so would not require any additional parameters in most numerical models, as the entrainment coefficient is already used to determine the flow velocity next to the ice face. Nonetheless, it would clarify the important processes driving ice melting and facilitate improved accuracy of such models.

6 Open Research

Unprocessed experimental parameters and measurements for the ice melting experiments are provided in the Supplementary Information. Measurements of the entrainment coefficient in Figure 3 are taken from McConnochie et al. (2021).

Acknowledgments

We gratefully acknowledge technical assistance from Anders Jensen. CDM thanks the Weston Howard Jr. Scholarship for funding. Support to CC was given by NSF project OCE-1434041 and OCE-1658079.

References

Cenedese, C., & Gatto, V. M. (2016). Impact of Two Plumes' Interaction on Submarine Melting of Tidewater Glaciers: A Laboratory Study. *J. Phys. Oceanogr.*, *46*, 361–367. doi: 10.1175/JPO-D-15-0171.1

Cenedese, C., & Linden, P. F. (2014). Entrainment in two coalescing axisymmetric turbulent plumes. *J. Fluid Mech.*, *752*, R2. doi: 10.1017/jfm.2014.389

Fried, M. J., Catania, G. A., Bartholomaus, T. C., Duncan, D., Davis, M., Stearns, L. A., . . . Sutherland, D. (2015). Distributed subglacial discharge drives significant submarine melt at a Greenland tidewater glacier. *Geophys. Res. Lett.*, *42*, 9328–9336. doi: 10.1002/2015GL065806

Jenkins, A. (2011). Convection-Driven Melting near the Grounding Lines of Ice Shelves and Tidewater Glaciers. *J. Phys. Oceanogr.*, *41*, 2279–2294. doi: 10.1175/JPO-D-11-03.1

Josberger, E. G. (1980). The effect of bubbles released from a melting ice wall on the melt-driven convection in salt water. *J. Phys. Oceanogr.*, *10*, 474-477. doi: 10.1175/1520-0485

Kaye, N. B., & Linden, P. F. (2004). Coalescing axisymmetric turbulent plumes. *J. Fluid Mech.*, *502*, 41–63. doi: 10.1017/S0022112003007250

Kerr, R. C., & McConnochie, C. D. (2015). Dissolution of a vertical solid surface by turbulent compositional convection. *J. Fluid Mech.*, *765*, 211–228. doi: 10.1017/jfm.2014.722

Mankoff, K. D., Straneo, F., Cenedese, C., Das, S. B., Richards, C. G., & Singh, H. (2016). Structure and dynamics of a subglacial discharge plume in a Greenlandic fjord. *J. Geophys. Res. Oceans*, *121*, 8670–8688. doi: 10.1002/2016JC011764

McConnochie, C. D., Cenedese, C., & Mcelwaine, J. N. (2021). Entrainment into particle-laden turbulent plumes. *Phys. Rev. Fluids*, *6*, 123502. doi: 10.1103/PhysRevFluids.6.123502

McConnochie, C. D., & Kerr, R. C. (2017a). Enhanced ablation of a vertical ice face due to an external freshwater plume. *J. Fluid Mech.*, *810*, 429–447. doi: 10.1017/jfm.2016.761

McConnochie, C. D., & Kerr, R. C. (2017b). Testing a common ice-ocean parameterization with laboratory experiments. *J. Geophys. Res. Oceans*, *122*, 5905–5915. doi: 10.1002/2017JC012918

Mingotti, N., & Woods, A. W. (2019). Multiphase plumes in a stratified ambient. *J. Fluid Mech.*, *869*, 292–312. doi: 10.1017/jfm.2019.198

Morton, B. R., Taylor, G. I., & Turner, J. S. (1956). Turbulent gravitational convection from maintained and instantaneous sources. In *Proceedings of the royal society a: Mathematical, physical and engineering sciences* (Vol. 234, pp. 1–23).

Nienow, P. W. (2017). Recent Advances in Our Understanding of the Role of Meltwater in the Greenland Ice Sheet System. *Curr. Clim. Change Rep.*, *3*, 330–344. doi: 10.1007/s40641-017-0083-9

Pritchard, H. D., Arthern, R. J., Vaughan, D. G., & Edwards, L. A. (2009). Extensive dynamic thinning on the margins of the Greenland and Antarctic ice sheets. *Nature*, *461*, 971–975. doi: 10.1038/nature08471

Richardson, J., & Hunt, G. R. (2022). What is the entrainment coefficient of a pure turbulent line plume? *J. Fluid Mech.*, *934*, A11. doi: 10.1017/jfm.2021.1070

Rignot, E., Jacobs, S., Mouginot, J., & Scheuchl, B. (2013). Ice shelf melting around Antarctica. *Science*, *341*, 266–270. doi: 10.1126/science.1235798

Slater, D. A., Nienow, P. W., Cowton, T. R., Goldberg, D. N., & Sole, A. J. (2015). Effect of near-terminus subglacial hydrology on tidewater glacier submarine melt rates. *Geophys. Res. Lett.*, *42*, 2861–2868. doi: 10.1002/2014GL062494

Straneo, F., & Cenedese, C. (2015). The dynamics of Greenland's glacial fjords and their role in climate. *Annu. Rev. Mar. Sci.*, *7*, 89–112. doi: 10.1146/annurev-marine-010213-135133

Sutherland, B. R., Rosevear, M. G., & Cenedese, C. (2020). Laboratory experiments modeling the transport and deposition of sediments by glacial plumes rising under an ice shelf. *Phys. Rev. Fluids*, *5*(1), 13802. doi: 10.1103/PhysRevFluids.5.013802

Wells, A. J., & Worster, M. G. (2008). A geophysical-scale model of vertical natural convection boundary layers. *J. Fluid Mech.*, *609*, 111–137. doi: 10.1017/jfm.2021.1070

Supporting Information for "Increased Melting of Marine-Terminating Glaciers by Sediment-Laden Plumes"

C. D. McConnochie[1]and C. Cenedese[2]

[1]Department of Civil and Natural Resources Engineering, University of Canterbury

[2]Physical Oceanography Department, Woods Hole Oceanographic Institution

Contents of this file

Corresponding author: C. D. McConnochie, Department of Civil and Natural Resources Engineering, University of Canterbury, New Zealand. (craig.mcconnochie@canterbury.ac.nz)

Table S1. Unprocessed measurements from laboratory experiments from which all derived quantities can be calculated. Parameters are: ambient fluid density (ρ_a), source fluid density (ρ_s), ambient fluid temperature (T_a), source fluid temperature (T_s), ambient fluid depth (H), source sediment concentration by weight (ϕ), source flow rate (Q), initial ice mass (M_i), final ice mass (M_f), and duration of experiment (t).

Experiment	ρ_a	ρ_s	T_a	T_s	H	ϕ	Q	M_i	M_f	t
	$\mathrm{kg\,m^{-3}}$	$\mathrm{kg\,m^{-3}}$	°C	°C	m	%	$\mathrm{ml\,s^{-1}}$	g	g	min
A	1022.015	998.865	3.2	0.5	0.25	0.00	6.0	4260	4202	6.0
B	1021.883	998.787	3.0	0.5	0.26	0.00	6.0	4186	4120	6.0
C	1022.235	998.765	3.1	1.2	0.26	1.00	6.0	4308	4236	4.5
D	1021.987	998.656	3.0	0.9	0.26	0.50	6.0	4254	4186	4.5
E	1022.264	998.6	3.0	0.7	0.27	0.25	6.0	4322	4260	4.5
F	1022.060	998.6	3.0	1.0	0.27	0.75	6.0	4390	4316	4.5
G	1022.585	998.6	3.2	0.7	0.27	1.25	6.0	4170	4094	4.5
H	1021.935	998.861	3.1	1.0	0.26	1.50	6.0	4328	4262	4.5